Environmental Science and Pollution Research (2018) 25:19403–19412
https://doi.org/10.1007/s11356-018-2141-9

RESEARCH ARTICLE

Distribution and health risks of aerosol black carbon in a representative city of the Qinghai-Tibet Plateau

Jun Wu[1,2] · Jian Lu[3] · Xiuyun Min[1,2] · Zhenhua Zhang[4]

Received: 17 December 2017 / Accepted: 25 April 2018 / Published online: 4 May 2018

Abstract

Although aerosol black carbon (BC) exerts strong influences on human health, research on potential health risks of aerosol BC around the Qinghai-Tibet Plateau is very limited. This is the very first study to investigate the distribution of aerosol BC in a typical city of the Qinghai-Tibet Plateau and the resulting health risks. The results showed that the maximal real-time (5-min monitoring interval) concentration of aerosol BC was 22.34 μg/m^3, much higher than day- and week-averaged concentrations which were in the range of 1.28–6.15 and 1.93–4.63 μg/m^3, respectively. The health risks were evaluated using four different health endpoints including low birth weight (LBW), percentage lung function decrement of school-aged children (PLFD), cardiovascular mortality (CM), and lung cancer (LC). The highest risks of LBW, PLFD, CM, and LC had reached 69.5, 184.4, 67.4, and 31.8 numbers of equivalent passively smoked cigarettes (PSC), respectively. The concentrations and health risks of aerosol BC in the study area are at a middle level among the global cities/regions. In comparison, the cities of the Qinghai-Tibet Plateau are experiencing high potential health risks resulting from aerosol BC to need more effective prevention and control of air pollution.

Keywords Aerosol black carbon · The Qinghai-Tibet Plateau · Distribution · Health risk

Introduction

Black carbon (BC), an important atmospheric aerosol that can deposit on environmental matrices, is generally created by weathering of graphitic carbon in rocks (Dickens et al. 2004) and the incomplete combustion of fossil fuels, vegetation, biofuels, and biomass (Cochrane 2003; Zhang and Wang 2011). BC generally possesses characteristics including high specific surface areas, variable particle size ranging from nanometers to mircometers, and a three-dimensional structure made up of stacked aromatic sheets (Koelmans et al. 2006). BC has been paid more attention due to its non-negligible contributions to global warming (Ramanathan and Carmichael 2008), strong relationship with persistent organic pollutants (Ni et al. 2014), and strong influences on human health (Koelmans et al. 2006; Shrestha et al. 2010).

The Qinghai-Tibet Plateau, covering a total area of approximately 3.0×10^6 km^2 (about 2.5×10^6 km^2 in China), has been called the "last pure land" in China because of its high elevation and relatively severe natural conditions to prevent extensive anthropogenic activities. However, inorganic pollutants such as heavy metals and various organic pollutants have been frequently detected in different matrices of this area, exerting potential risks to the ecosystem and human health (Wu et al. 2016a, b).

Several recent studies on aerosol BC around the Qinghai-Tibet Plateau have been performed (Babu et al. 2011; Marinoni et al. 2010; Wang et al. 2016; Zhao et al. 2012).

Responsible editor: Philippe Garrigues

Electronic supplementary material The online version of this article (https://doi.org/10.1007/s11356-018-2141-9) contains supplementary material, which is available to authorized users.

✉ Jian Lu
jlu@yic.ac.cn

[1] Key Laboratory of Comprehensive and Highly Efficient Utilization of Salt Lake Resources, Qinghai Institute of Salt Lakes, Chinese Academy of Sciences, Xining, Qinghai 810008, China

[2] Qinghai Provincial Key Laboratory of Geology and Environment of Salt Lakes, Xining, Qinghai 810008, China

[3] Key Laboratory of Coastal Environmental Processes and Ecological Remediation, Yantai Institute of Coastal Zone Research, Chinese Academy of Sciences, Yantai, Shandong 264003, China

[4] School of Resources and Environmental Engineering, Ludong University, Yantai, Shandong 264025, China

The concentrations of aerosol BC are variable in different regions. Ma et al. (2003) investigated the concentrations of aerosol BC at Waliguan Observatory that is located on the top of Mt. Waliguan (an important mountain of the Qinghai-Tibet Plateau). The average concentration was 0.272 μg/m^3. Cao et al. (2010) measured the concentrations of aerosol BC around the southeastern Qinghai-Tibet Plateau along the valley of the Yarlung Tsangpo River during winter. The average concentration of BC was 0.75 μg/m^3 which was significantly higher than the background concentrations (0.004–0.34 μg/m^3) that were measured in the global background and remote regions. Ming et al. (2010) collected air and precipitation samples from Nam Co region of central Tibet. The highest concentration of BC in air and precipitation samples reached 0.239 μg/m^3 and 2158 μg/kg, respectively. Dumka et al. (2010) found that the concentrations of BC in a site of the Central Mt. Everest (29.4° N, 79.5° E) showed seasonal variations with the average value of 0.99 μg/m^3. Engling et al. (2011) reported that the concentrations of aerosol BC at a monitoring station (25.01° N, 98.30° E) in Tengchong (located on the southeastern edge of the Qinghai-Tibet Plateau) varied from 0.043 to 1.471 μg/m^3. It was also found that the concentrations of aerosol BC around cities/regions with a high population were significantly higher. Zhu et al. (2017) reported that the highest concentration of BC at an urban site in Lhasa (29.6° N, 91.1° E) and a remote site in Lulang (29.76° N, 94.73° E) reached 7.68 and 2.20 μg/m^3, respectively. Moreover, some results showed that the concentrations of aerosol BC were affected by different factors such as altitude and meteorological conditions (Mao and Liao 2016; Zhao et al. 2017).

Aerosol BC poses potential risks to the human health (Koelmans et al. 2006; Louwies et al. 2015; Shrestha et al. 2010). BC has been reported to be an important cause for several human cardiovascular and respiratory diseases (Koelmans et al. 2006). Blood pressure increases when exposure concentration of BC increases, which potentially induces cardiovascular morbidity and mortality (Louwies et al. 2015). It is also found that particle size of BC is in a close relationship with its harmful effects (Ni et al. 2014; Shrestha et al. 2010). To the best of our knowledge, the information on the health risks posed by BC especially around the Qinghai-Tibet Plateau has been very limited until now. Therefore, it is necessary to perform research work on the health risks posed by aerosol BC of the Qinghai-Tibet Plateau. This study performed a series of experiments to explore the distribution of aerosol BC around a typical city of the Qinghai-Tibet Plateau and evaluate the potential health risks posed by aerosol BC. The objective of this study is to provide comprehensive information on the aerosol BC and its adverse side, especially in the high-elevation regions such as the Qinghai-Tibet Plateau.

Materials and methods

Study area and aerosol BC monitoring strategy

Xining, the capital city of Qinghai Province and a representative city of the Qinghai-Tibet Plateau, was selected as the study area (Fig. S1). As the economic, political, and cultural center of Qinghai Province, Xining is also one of the most advanced and populated cities in the Qinghai-Tibet Plateau. Xining covers a total area of 7424 km^2 but only with 4.7% of urban region (Tan et al. 2017). The population of Xining in 2013 was 2.268 million (Tan et al. 2017).

Serving as landmark sites of Xining, a total seven sites were selected as target monitoring sites (Fig. S1). Near a coach station, Site XR is located at Xinning Road that bears heavy daily traffic. The daily amount of vehicles circulating on Site XR reached 44,000, and 80% of vehicles were gasoline-engine cars based on our observation and estimation. Site CP is situated at Center Plaza that is the local traffic hub of Xining. The daily amount of vehicles circulating on Site CP reached 53,000, and 75% of vehicles were gasoline-engine cars. Site QU is located at Qinghai University campus that is suburb of Xining. Sites RS and XA are situated at railway station and airport, respectively. The daily amount of vehicles circulating on the adjacent streets of Sites RS and XA reached 62,000 and 28,000, respectively. The gasoline-engine cars on streets near Sites RS and XA accounted for approximately 75 and 90% of the total vehicles, respectively. Site GIP is seated at Ganhe Industrial Park that consists of many factories and companies. The distance between Site GIP and the nearest industrial stack is approximately 3000 m and this factory has been closed. Site DC is located in Datong County (a county that belongs to Xining) and near Datong aluminum factory which is an important enterprise of Qinghai Province. The distance between Site DC and the industrial stacks is approximately 500 m.

Monitoring of aerosol BC was performed from 21 February 2017 to 20 May 2017. Four time intervals including morning (7:30–9:00), noon-afternoon (12:00–14:00), afternoon (17:30–18:30), and evening (21:30–22:30) were chosen for BC monitoring because these time intervals represent the typical work-life pace of Xining. Each sampling site was monitored for a whole week in one monitoring experiment because of very limited in situ monitoring device.

A microAeth AE51 real-time monitor (Aethlab Inc., San Francisco, CA, USA) was used to in situ monitor the concentrations of aerosol BC. The air sample was collected on T60 Teflon coated glass fiber filter strip and the concentration of aerosol BC was determined using the 880-nm optical absorption. The data of BC concentrations were recorded real timely by AE51 monitor and exported by the computer workstation connected with AE51 monitor. The flow rate was set at 100 mL/min for all monitoring experiments. The time interval

of AE51 measurements was set as 5 min. A total of 490 data regarding real-time (5-min monitoring interval) concentration of BC were obtained at each monitoring site.

The comparison on concentrations of BC at different sites or within different time intervals or days was evaluated by analysis of variance (ANOVA) with calculation of the least significant differences (LSD, $P = 0.01$).

Health risk assessment

Although aerosol BC is in a close relationship with several human cardiovascular and respiratory diseases and poses potential health risks to the public, the standard method for evaluating the health risks of BC has not yet been established. It might be feasible to use the equivalent numbers of passively smoked cigarettes (PSC) to express the health risks posed by aerosol BC since it is an airborne pollutant. Targeting at aerosol BC, a health risk assessment method based on environmental tobacco smoke (ETS) has been developed by van der Zee et al. (2016). The present study also used this method to evaluate the health risks posed by aerosol BC of Xining.

Four health endpoints including low birth weight (LBW) denoting a birth weight < 2.5 kg after 37-week gestation, percentage lung function decrement of school aged children (PLFD), cardiovascular mortality (CM), and lung cancer (LC) were selected to evaluate the health risks according to van der Zee et al. (2016). The equivalent amounts of PSC (N_{psc}) can be calculated as follows:

$$N_{psc} = \frac{\beta_{BC}}{\beta_{cigarette}} \times \Delta C = \frac{\frac{\ln(RR_{BC})}{\Delta concentartion}}{\frac{\ln(RR_{ETS})}{N_a}} \times \Delta C$$

where $\beta_{BC} = \frac{\ln(RR_{BC})}{\Delta concentration}$, is the regression coefficient per 1 μg/m^3 of BC; $\beta_{cigarette} = \frac{\ln(RR_{ETS})}{N_a}$, is the regression coefficient per cigarette; $\Delta concentration = 1$ μg/m^3 for BC; ΔC refers to the difference between the monitored and background concentrations of aerosol BC; RR_{BC} is relative risk for the association between BC and the health endpoint; RR_{ETS} means relative risk for ETS exposure; N_a represents the assumed number of cigarettes, which is 9 for children and 7 for adults according to van der Zee et al. (2016). A survey was performed to investigate the number of cigarettes smoked indoors by smokers in Xining. Approximately 550 smokers answered the questionnaires and they averagely smoke about 14 cigarettes per day. Therefore, the number of cigarettes smoked indoors assumed by van der Zee et al. (2016) is suitable for this study. Values of RR_{BC} and RR_{ETS} can be obtained from van der Zee et al. (2016). Xining lies approximately 90 km to the northeast of Waliguan Observatory that is relatively isolated from anthropogenic activities (Ma et al. 2003). Therefore, the background concentration of BC in this study was chosen as 0.272 μg/m^3 (data from Waliguan Observatory based on Ma et al. 2003).

Differences in health risks of BC at different sites or within different time intervals or days were determined by ANOVA ($p = 0.01$).

Results and discussion

Distribution of aerosol BC in the study area

Aerosol BC was monitored with four time intervals in a day as described above, and on each day during a week so as to obtain 490 data for each monitoring site (Fig. S2). The statistical distribution of BC concentrations was shown by box plots in Fig. 1 and Figs. S3 and S4. Concentrations of aerosol BC at different sites showed significant difference according to ANOVA results ($P < 0.01$). Concentrations of BC at the same site varying with four time intervals or 7 days also exhibited significant difference based on ANOVA results ($p < 0.01$). Site DC possessed the highest week-averaged concentration of BC (4.63 μg/m^3) with standard deviation of 3.18 μg/m^3 while Site XA showed the lowest value of 1.93 μg/m^3 (Fig. 1). The week-averaged concentrations of BC at the rest 5 sites ranged from 1.99 to 3.72 μg/m^3 (Fig. 1). For each site, concentrations of aerosol BC showed large fluctuations during the whole week. On Monday, the real-time (5-min monitoring interval) concentration of BC at Site DC reached the maximum value of 22.34 μg/m^3. In comparison, the real-time concentration of BC reached its minimum value of 0.40 μg/m^3 at Site QU on Sunday (Fig. S2).

Concentrations of aerosol BC at different sites varied significantly and depended on each day of a whole week (Fig.

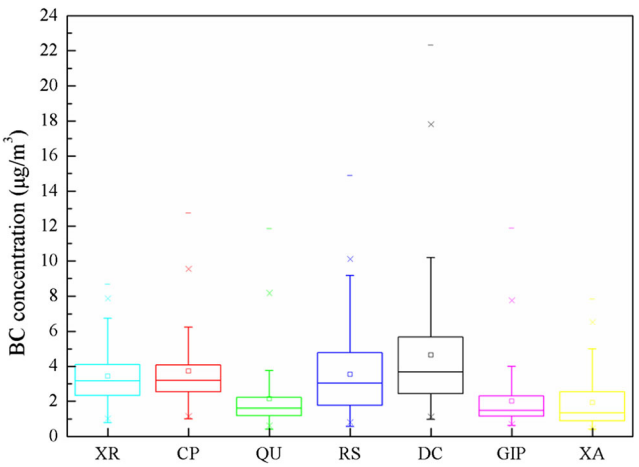

Fig. 1 Box plots of concentrations of aerosol black carbon (BC) at seven monitoring sites. In each box, the bottom and top of the box illustrate the 25th and 75th percentiles; the mid-line of the box means the median value; the small box inside each box represents the average value; the bottom and top of the whiskers refers to the 10th and 90th percentiles; and the extreme values exceeding three times the 25th percentile are marked

S3). The minimal day-averaged concentration of BC at all sampling sites was 1.28 μg/m^3 (Site GIP). Except Wednesday and Friday, Site DC possessed the maximal day-averaged concentration of BC among all sites ranging from 4.39 to 6.15 μg/m^3 (Fig. S3). Among all sites, Sites CP and RS showed the maximal day-averaged concentration of BC with values of 4.94 and 5.35 μg/m^3 for Wednesday and Friday, respectively (Fig. S3). The maximal day-averaged concentration of BC at Sites XR, CP, QU, RS, DC, GIP, and XA occurred on Thursday, Wednesday, Thursday, Friday, Thursday, Monday, and Sunday with values of 4.06, 4.94, 2.77, 5.35, 6.15, 2.55, and 2.75 μg/m^3, respectively (Fig. S3).

The concentrations of BC at seven sites also varied with four time intervals (Fig. S4). In the morning, the time-interval-averaged concentrations of aerosol BC at seven sites reached the maximum values ranging from 3.02 to 6.13 μg/m^3. Site DC showed the maximal time-interval-averaged concentrations of aerosol BC in the morning, noon-afternoon, afternoon, and evening with the values of 6.13, 3.33, 4.58, and 5.01 μg/m^3, respectively.

Health risks of aerosol BC in the study area

Aerosol BC is closely associated with several human cardiovascular and respiratory diseases to pose potential risks to the human health (Koelmans et al. 2006; Louwies et al. 2015; Shrestha et al. 2010). Health risk assessment model was developed by van der Zee et al. (2016) to use four health endpoints including LBW, PLFD, CM, and LC for exploring potential health risks posed by aerosol BC. Therefore, health risks posed by aerosol BC of this study area were also evaluated by LBW, PLFD, CM, and LC, expressed into equivalent numbers of PSC (Figs. 2, 3, 4, and 5). Health risks posed by aerosol BC at different sites showed significant difference based on ANOVA results ($p < 0.01$). Health risks posed by aerosol BC at the same site varying with different time intervals or days also illustrated significant difference according to ANOVA results ($p < 0.01$).

Similar to concentration pattern, health risks of LBW calculated by real-time concentrations of BC at Site DC reached the maximal value with 69.5 equivalent numbers of PSC while that at Site QU showed the lowest value of 0.4 (Fig. 2). The week-averaged risks of LBW at seven sites ranged from 5.2 (Site XA) to 13.7 (Site DC) equivalent numbers of PSC. Day-averaged risks of LBW at Site DC reached the highest values varying from 13.0 to 18.5 equivalent numbers of PSC on each day of a week except Wednesday and Friday while Sites XA, GIP, and QU possessed the minimal day-averaged risks of LBW, showing significant difference in day-averaged risks (Fig. S5). The highest time-interval-averaged risks of LBW occurred in the morning for all seven sites ranging from 8.7 to 18.5 equivalent numbers of PSC whereas Site DC possessed the highest time-interval-averaged risks of LBW in the morning, noon-afternoon, afternoon, and evening with the values of 18.5, 9.6, 13.6, and 14.9 equivalent numbers of PSC, respectively (Fig. S6). The minimal time-interval-averaged risks of LBW usually occurred in the time intervals of noon-afternoon and afternoon (Fig. S6).

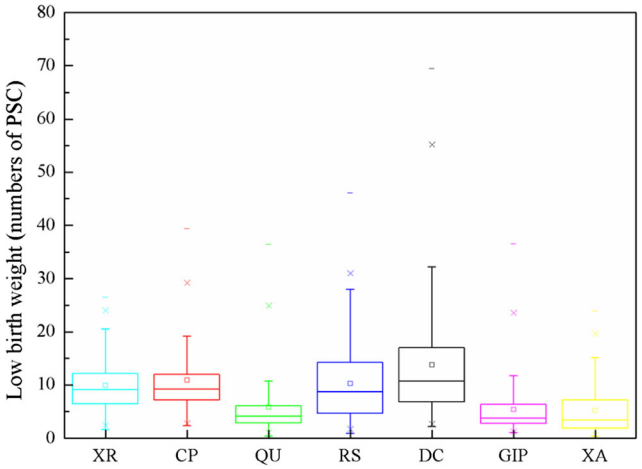

Fig. 2 Box plots of health risks expressed by low birth weight at seven monitoring sites. The health risks expressed by low birth weight were measured using equivalent numbers of passively smoked cigarettes (PSC). In each box, the bottom and top of the box illustrate the 25th and 75th percentiles; the mid-line of the box means the median value; the small box inside each box represents the average value; the bottom and top of the whiskers refers to the 10th and 90th percentiles; and the extreme values exceeding three times the 25th percentile are marked

The week-averaged health risks of PLFD at 7 sites illustrated significant difference (Fig. 3). The highest health risks of PLFD occurred in Site DC on Monday with 184.4 equivalent numbers of PSC while Site QU showed the lowest risks of PLFD on Sunday with 1.1 (Fig. 3). The week-averaged risks

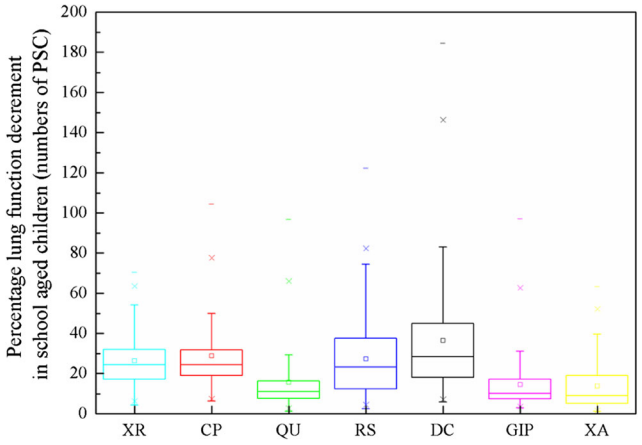

Fig. 3 Box plots of health risks expressed by percentage lung function decrement of school-aged children at seven monitoring sites. The health risks expressed by percentage lung function decrement of school-aged children were measured using equivalent numbers of passively smoked cigarettes (PSC). In each box, the bottom and top of the box illustrate the 25th and 75th percentiles; the mid-line of the box means the median value; the small box inside each box represents the average value; the bottom and top of the whiskers refers to the 10th and 90th percentiles; and the extreme values exceeding three times the 25th percentile are marked

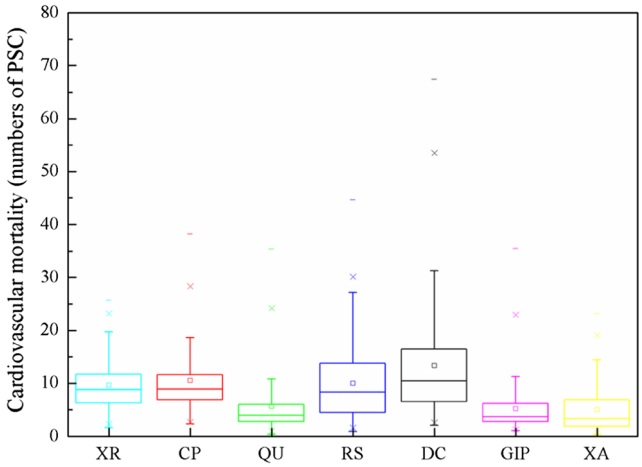

Fig. 4 Box plots of health risks expressed by cardiovascular mortality at seven monitoring sites. The health risks expressed by cardiovascular mortality were measured using equivalent numbers of passively smoked cigarettes (PSC). In each box, the bottom and top of the box illustrate the 25th and 75th percentiles; the mid-line of the box means the median value; the small box inside each box represents the average value; the bottom and top of the whiskers refers to the 10th and 90th percentiles; and the extreme values exceeding three times the 25th percentile are marked

of PLFD at seven sites ranged from 13.8 (Site XA) to 36.5 (Site DC) equivalent numbers of PSC, much higher than those of LBW (Figs. 2 and 3). Among seven sites during a week, Site DC showed the maximal day-averaged risks of PLFD with values in the range of 34.4–49.1 equivalent numbers of PSC on Monday, Tuesday, Thursday, Saturday, and Sunday while Sites CP and RS showed the maximal day-averaged risks of PLFD with values of 39.0 and 42.4 equivalent numbers of PSC on Wednesday and Friday, respectively, illustrating significant difference in day-averaged risks (Fig. S7). The

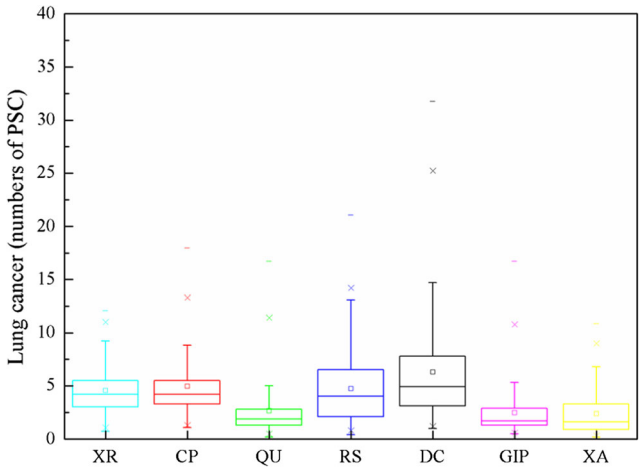

Fig. 5 Box plots of health risks expressed by lung cancer at seven monitoring sites. The health risks expressed by lung cancer were measured using equivalent numbers of passively smoked cigarettes (PSC). In each box, the bottom and top of the box illustrate the 25th and 75th percentiles; the mid-line of the box means the median value; the small box inside each box represents the average value; the bottom and top of the whiskers refers to the 10th and 90th percentiles; and the extreme values exceeding three times the 25th percentile are marked

maximal time-interval-averaged risks of PLFD occurred in the morning at all seven sites ranging from 23.0 to 49.0 equivalent numbers of PSC whereas Site DC possessed the maximal time-interval-averaged risks of PLFD in the morning, noon-afternoon, afternoon, and evening with the values of 49.0, 25.6, 36.0, and 39.6 equivalent numbers of PSC, respectively (Fig. S8).

Similar to LBW, the highest health risk of CM occurred at Site DC with 67.4 equivalent numbers of PSC while Site QU showed the lowest risk of CM with 0.4 (Fig. 4). The week-averaged risks of CM at seven sites ranged from 5.1 (Site XA) to 13.3 (Site DC) equivalent numbers of PSC (Fig. 4). Except Wednesday and Friday, Site DC illustrated the highest day-averaged risks of CM varying from 12.6 to 18.0 equivalent numbers of PSC while Sites XA, GIP, and QU showed the lowest day-averaged risks of CM, also exhibiting significant difference in day-averaged risks (Fig. S9). The maximal time-interval-averaged risks of CM at all seven sites occurred in the morning ranging from 8.4 (Site GIP) to 17.9 (Site DC) equivalent numbers of PSC whereas Site DC possessed the maximal average risks of CM in all four time intervals (Fig. S10). The minimal time-interval-averaged risks of CM usually occurred in the noon-afternoon and afternoon (Fig. S10).

Compared with other three endpoints, health risks of LC showed relatively low values. Health risks of LC reached the highest value of 31.8 equivalent numbers of PSC at Site DC while Site QU showed the minimal risk of LC with 0.2 (Fig. 5), less than half of the corresponding risks of LBW and CM. The week-averaged risks of LC risks at seven sites ranged from 2.4 (Site XA) to 6.3 (Site DC) equivalent numbers of PSC (Fig. 5). Among all sites, day-averaged risks of LC at Site DC reached the highest values varying from 5.9 to 8.5 equivalent numbers of PSC on each day of a week except Wednesday and Friday while day-averaged risks of LC reached the highest values of 6.7 (Sites CP) equivalent numbers of PSC on Wednesday and 7.3 (Site RS) on Friday, respectively (Fig. S11). The maximal time-interval-averaged risks of LC occurred in the morning for all seven sites ranging from 4.0 (Site GIP) to 8.4 (Site DC) equivalent numbers of PSC whereas Site DC possessed the maximal time-interval-averaged risks of LC for all four time intervals (Fig. S12). The minimal time-interval-averaged risks of LC usually occurred in the time intervals of noon-afternoon and afternoon (Fig. S12).

Comparison on health risks of aerosol BC in different sites of the world

Besides concentration data of aerosol BC in Xining, this study also cited concentration data of aerosol BC in other 42 cities/regions of 24 countries to make comparison on concentrations and potential health risks of BC in the study area and the other sites at a global scale (Table 1). The maximal concentration

Table 1 Health risks of BC expressed into equivalent numbers of passively smoked cigarettes in different sites of the world

Sampling sites	Country	Reference	Con[a]	LBW	PLFD	CM	LC
Xining	China	This study[b]	22.34	69.5	184.4	67.4	31.8
Xining	China	This study[c]	3.05	8.8	23.2	8.5	4.0
Xining	China	This studyd	2.51	7.1	18.7	6.8	3.2
Lhasa	China	Zhu et al. (2017)	7.68	23.3	61.9	22.6	10.7
Lulang	China	Zhu et al. (2017)	2.20	6.1	16.1	5.9	2.8
Beijing	China	Ji et al. (2017)	33.5	104.7	277.7	101.6	47.9
Shanghai	China	Wang et al. (2014)	28.42	88.7	235.2	86.0	40.5
Guangzhou	China	Chen et al. (2014)	20.5	63.7	169.0	61.8	29.1
Xi'an	China	Cao et al. (2009)	65.00	203.9	540.9	197.8	93.2
Hong Kong	China	Rakowska et al. (2014)	67.8	212.8	564.3	206.4	97.3
Tsukuba	Japan	Naoe et al. (2009)	7.20	21.8	57.9	21.2	10.0
Incheon City	Korea	Yoo et al. (2011)	20.82	64.7	171.7	62.8	29.6
Karachi	Pakistan	Dutkiewicz et al. (2009)	40.00	125.2	332.0	121.4	57.2
Delhi	India	Srivastava et al. (2014)	24.00	74.8	198.3	72.5	34.2
Kolkata	India	Pani and Verma (2014)	73.00	229.1	607.8	222.3	104.7
New York City	USA	Patel et al. (2009)	5.50	16.5	43.7	16.0	7.5
Los Angeles	USA	Krasowsky et al. (2016)	0.64	1.2	3.1	1.1	0.5
Las Vegas	USA	Vedantham et al. (2012)	1.97	5.3	14.2	5.2	2.4
CRG	USA	Jaffe et al. (2015)	88.9	279.2	740.7	270.9	127.6
San Ysidro	USA	Quintana et al. (2014)	5.70	17.1	45.4	16.6	7.8
El Paso	USA	Raysoni et al. (2011)	1.74	4.6	12.3	4.5	2.1
Montreal	Canada	Weichenthal et al. (2014)	9.46	28.9	76.8	28.1	13.2
Ontario	Canada	Healy et al. (2017)	1.74	4.6	12.3	4.5	2.1
Ciudad Juárez	Mexico	Raysoni et al. (2011)	5.54	16.6	44.0	16.1	7.6
Tijuana	Mexico	Takahama et al. (2014)	21.00	65.3	173.2	63.4	29.9
Kingston	Jamaica	Boman and Gaita (2015)	7.00	21.2	56.2	20.6	9.7
São Paulo	Brazil	Castanho and Artaxo (2001)	7.60	23.1	61.2	22.4	10.6
Piracicaba	Brazil	Lara et al. (2005)	4.20	12.4	32.8	12.0	5.7
Gotuzo	Chile	Artaxo et al. (1999)	10.40	31.9	84.6	31.0	14.6
Las Condes	Chile	Artaxo et al. (1999)	3.50	10.2	27.0	9.9	4.6
Paris	French	Ruellan and Cachier (2001)	49.00	153.5	407.2	148.9	70.2
Granada	Spain	Lyamani et al. (2011)	8.60	26.2	69.6	25.5	12.0
Milan	Italy	Invernizzi et al. (2011)	6.30	19.0	50.4	18.4	8.7
Stockholm	Sweden	Krecl et al. (2017)	2.10	5.8	15.3	5.6	2.6
Helsinki	Finland	Viidanoja et al. (2002)	2.20	6.1	16.1	5.9	2.8
Ny-Ålesund	Norway	Markowicz et al. (2017)	0.44	0.5	1.4	0.5	0.2
Auckland	New Zealand	Wang and Shooter (2005)	3.42	9.9	26.3	9.6	4.5
Suva	Fiji	Isley et al. (2017)	4.90	14.6	38.7	14.1	6.7
Nairobi	Kenya	Gatari and Boman (2003)	4.00	11.7	31.2	11.4	5.4
Nanyuki	Kenya	Gatari and Boman (2003)	1.10	2.6	6.9	2.5	1.2
Meru	Kenya	Gatari and Boman (2003)	2.40	6.7	17.8	6.5	3.1
Dakar	Senegal	Doumbia et al. (2012)	15.40	47.7	126.4	46.2	21.8
Bamako	Mali	Doumbia et al. (2012)	19.20	59.6	158.2	57.9	27.3
Yaounde	Cameroon	Doumbia et al. (2012)	2.40	6.7	17.8	6.5	3.1
Cotonou	Benin	Doumbia et al. (2012)	4.90	14.6	38.7	14.1	6.7

CRG, Columbia River Gorge; LBW, low birth weight; PLFD, percentage lung function decrement in school aged children; CM, cardiovascular mortality; LC, lung cancer

[a] BC concentration with unit of micrograms per cubic meter

[b] Peak concentration of BC reported by this study

[c] Average concentration of BC reported by this study

[d] Median concentration of BC reported by this study

was generally chosen unless only average or individual concentration was shown in the references. Interestingly, USA showed the highest (Columbia River Gorge, abbreviated as CRG) concentration of BC with a value of 88.90 μg/m^3 while Norway illustrated the lowest concentration (Ny-Ålesund) with 0.64 μg/m^3. BC concentrations in several cities of China, Korea, Pakistan, India, Mexico, Chili, French, Senegal, and Mali exceeded 10 μg/m^3, much higher than those in other cities/regions (Table 1). The concentrations of aerosol BC in Xining were lower than those of Shanghai, Xi'an, Karachi, Delhi, Kolkata, CRG, and Paris.

To our knowledge, criterion for evaluating pollution by aerosol BC has not been established. Compared with other cities around the world, concentration of aerosol BC in Xining was at middle level, not very high or low enough, even among the cities of the Qinghai-Tibet Plateau (Table 1). However, the highest concentration of aerosol BC in this study area reached 22.34 μg/m^3, still suggesting urgent need for air pollution control. Large amounts of small hydrocarbon molecules and polycyclic aromatic hydrocarbons (PAHs) are produced during the formation of BC particles (Ni et al. 2014). BC particles carrying PAHs react with chlorine to produce polychlorinated biphenyls (PCBs), polychlorinated dibenzo-para-dioxins (PCDDs), and polychlorinated dibenzofurans (PCDFs) when chlorine presents during combustion (Ni et al. 2014). Due to a close relationship with persistent organic pollutants and human health, criterion establishment for assessing aerosol BC pollution should be put on the agenda as soon as possible.

There are not standard protocols for evaluating health risks of aerosol BC up to now. Therefore, a recently published method was selected to assess health risks of BC by using equivalent numbers of PSC in this study. Health risks posed by aerosol BC were expressed into four health endpoints so as to obtain comprehensive evaluation.

The maximal health risks of CRG reached 279.2, 740.7, 270.9, and 127.6 equivalent numbers of PSC for LBW, PLFD, CM, and LC, respectively. Ny-Ålesund showed the minimal health risks of LBW, PLFD, CM, and LC with 0.5, 1.4, 0.5, and 0.2 equivalent numbers of PSC, respectively. In Asia, India showed the most serious air pollution with BC concentration of 73.00 μg/m^3, thus exerting health risks of LBW, PLFD, CM, and LC with 229.1, 607.8, 222.3, and 104.7 equivalent numbers of PSC, respectively. Besides USA, Canada in North America also showed relatively high health risks of LBW, PLFD, CM, and LC with 28.9, 76.8, 28.1, and 13.2 equivalent numbers of PSC. In terms of South America, Chili showed the highest health risks with 31.9, 84.6, 31.0, and 14.6 equivalent numbers of PSC for LBW, PLFD, CM, and LC, respectively. Among European countries, France exhibited the maximal health risks of LBW, PLFD, CM, and LC with 153.5, 407.2, 148.9, and 70.2 equivalent numbers of PSC, respectively. Fiji and Mali possessed the highest health risks of LBW/PLFD/CM/LC in Oceania and Africa, respectively, with 14.6/38.7/14.1/6.7 and 59.6/158.2/57.9/27.3 equivalent numbers of PSC, respectively.

Based on evaluation results, most of the cities (even for the cities located in the Qinghai-Tibet Plateau) around the world are experiencing the high health risks posed by aerosol BC (Table 1). Health risks of BC in Xining were lower than those in Shanghai, Xi'an, Karachi, Delhi, Kolkata, CRG, and Paris. Although more new methods are waiting to be developed for more precisely and comprehensively evaluating health risks of BC, the current results still suggest the needs for effective control of aerosol BC.

Possible factors affecting concentrations of aerosol BC in the study area

Industrial production contributes to concentrations of aerosol BC to a great extent. Site DC showed significantly higher concentrations of BC, which may be due to the nearby aluminum factory emission. Out of our expectation, concentrations of BC at Site GIP exhibited relatively normal values, which might be attributed to that over 70% of enterprises in this industrial park have been in stopping-production status since 2016. Therefore, distribution features of BC at Sites DC and GIP illustrate that anthropogenic activities such as industrial production and mining will contribute to concentrations of aerosol BC, which is also proved by Jaffe et al. (2015).

The traffic might be another important factor contributing to the concentrations of BC. Except Site DC, the highest concentrations of BC at the rest sites mainly occurred in the morning (exceeding 4 days out of a week), especially during workday. Vehicle exhaust, especially during rush hours, might offer concentrations of BC to great extent, which is also similar to the findings of other scientists (Chen et al. 2014; Dutkiewicz et al. 2009; Ji et al. 2017; Patel et al. 2009; Rakowska et al. 2014). Aircrafts and trains are mainly used for inter-province transportation. Many flights and trains are arranged to depart in the morning, noon or early afternoon so that people have to arrive at airport or railway station by cars, taxi or bus in the morning. Therefore, it is reasonable that the highest concentrations of aerosol BC at Sites RS and XA occurred in the morning. Located on the arterial road and local traffic hub, the highest concentrations of aerosol BC at Sites XR and CP reflect the local life-work schedules that include commuting for work (workday morning and afternoon), morning market-shopping (weekend morning), and evening leisure. Interestingly, the highest real-time concentrations of aerosol BC at Site QU mainly occurred in the morning (4 days out of a week) and noon (3 days out of a week), which might be affected by other sources such as restaurant cooking besides traffic.

Conclusions

A total of seven sites of Xining were monitored a week with four time intervals of each day to obtain concentrations of aerosol BC. The real-time (5-min monitoring interval) concentrations of BC in the study area ranged from 0.40 to 22.34 μg/m^3 while the day-averaged and week-averaged concentrations of BC were in the range of 1.28–6.15 and 1.93–4.63 μg/m^3, respectively. The highest time-interval-averaged concentrations of BC at seven sites occurred in the morning of each day. The health risks posed by aerosol BC were evaluated using LBW, PLFD, CM, and LC, with the highest values of 69.5, 184.4, 67.4, and 31.8 equivalent numbers of PSC, respectively. To the best of our knowledge, this is the first report on the health risks posed by BC in the Qinghai-Tibet Plateau. The health risks of BC showed the same pattern with concentration. Compared with other cities/regions around the world, the concentrations and health risks of BC in Xining were at the middle level. However, Xining and other cities of the Qinghai-Tibet Plateau are still experiencing high potential health risks posed by aerosol BC based on evaluation results to need effective prevention and control of air pollution.

Acknowledgements The authors would like to thank Dr. Yang Liu at The University of Western Ontario for polishing the manuscript. The authors would like to thank the reviewers for their valuable suggestions and comments on the manuscript.

Funding information This work was supported by One Hundred Talents Program of Chinese Academy of Sciences (Grant numbers of Y610061033 and Y629041021), National Natural Science Foundation of China (No. 41671319), Thousand Talents Plan of Qinghai Province (Y740171071), and Two-Hundred Talents Plan of Yantai (Y739011021).

References

Artaxo P, Oyola P, Martinez R (1999) Aerosol composition and source apportionment in Santiago de Chile. Nucl Instrum Meth B 150:409–416. https://doi.org/10.1016/S0168-583X(98)01078-7

Babu SS, Chaubey JP, Moorthy KK, Gogoi MM, Kompalli SK, Sreekanth V, Bagare SP, Bhatt BC, Gaur VK, Prabhu TP, Singh NS (2011) High altitude (~4520 m amsl) measurements of black carbon aerosols over western trans-Himalayas: seasonal heterogeneity and source apportionment. J Geophys Res 116:D24201. https://doi.org/10.1029/2011JD016722

Boman J, Gaita SM (2015) Mass, black carbon and elemental composition of $PM_{2.5}$ at an industrial site in Kingston, Jamaica. Nucl Instrum Meth B 363:131–134. https://doi.org/10.1016/j.nimb.2015.08.068

Cao J-J, Zhu C-S, Chow JC, Watson JG, Han Y-M, Wang G, Shen Z, An Z-S (2009) Black carbon relationships with emissions and meteorology in Xi'an, China. Atmos Res 94:194–202. https://doi.org/10.1016/j.atmosres.2009.05.009

Cao J, Tie X, Xu B, Zhao Z, Zhu C, Li G, Liu S (2010) Measuring and modeling black carbon (BC) contamination in the SE Tibetan Plateau. J Atmos Chem 67:45–60. https://doi.org/10.1007/s10874-011-9202-5

Castanho ADA, Artaxo P (2001) Wintertime and summertime São Paulo aerosol source apportionment study. Atmos Environ 35:4889–4902. https://doi.org/10.1016/S1352-2310(01)00357-0

Chen X, Zhang Z, Engling G, Zhang R, Tao J, Lin M, Sang X, Chan C, Li S, Li Y (2014) Characterization of fine particulate black carbon in Guangzhou, a megacity of South China. Atmos Pollut Res 5:361–370. https://doi.org/10.5094/APR.2014.042

Cochrane MA (2003) Fire science for rainforests. Nature 421:913–919. https://doi.org/10.1038/nature01437

Dickens AF, Gelinas Y, Masiello CA, Wakeham S, Hedges JI (2004) Reburial of fossil organic carbon in marine sediments. Nature 427:336–339. https://doi.org/10.1038/nature02299

Doumbia EHT, Liousse C, Galy-Lacaux C, Ndiaye SA, Diop B, Ouafo M, Assamoi EM, Gardrat E, Castera P, Rosse R, Akpo A, Sigha L (2012) Real time black carbon measurements in West and Central Africa urban sites. Atmos Environ 54:529–537. https://doi.org/10.1016/j.atmosenv.2012.02.005

Dumka U, Moorthy KK, Kumar R, Hegde P, Sagar R, Pant P, Singh N, Babu SS (2010) Characteristics of aerosol black carbon mass concentration over a high altitude location in the Central Himalayas from multi-year measurements. Atmos Res 96:510–521. https://doi.org/10.1016/j.atmosres.2009.12.010

Dutkiewicz VA, Alvi S, Ghauri BM, Choudhary MI, Husain L (2009) Black carbon aerosols in urban air in South Asia. Atmos Environ 43:1737–1744. https://doi.org/10.1016/j.atmosenv.2008.12.043

Engling G, Zhang Y-N, Chan C-Y, Sang X-F, Lin M, Ho K-F, Li Y-S, Lin C-Y, Lee JJ (2011) Characterization and sources of aerosol particles over the southeastern Tibetan Plateau during the Southeast Asia biomass-burning season. Tellus B 63:117–128. https://doi.org/10.1111/j.1600-0889.2010.00512.x

Gatari MJ, Boman J (2003) Black carbon and total carbon measurements at urban and rural sites in Kenya, East Africa. Atmos Environ 37:1149–1154. https://doi.org/10.1016/S1352-2310(02)01001-4

Healy RM, Sofowote U, Su Y, Debosz J, Noble M, Jeong C-H, Wang JM, Hilker N, Evans GJ, Doerksen G, Jones K, Munoz A (2017) Ambient measurements and source apportionment of fossil fuel and biomass burning black carbon in Ontario. Atmos Environ 161:34–47. https://doi.org/10.1016/j.atmosenv.2017.04.034

Invernizzi G, Ruprecht A, Mazza R, De Marco C, Močnik G, Sioutas C, Westerdahl D (2011) Measurement of black carbon concentration as an indicator of air quality benefits of traffic restriction policies within the ecopass zone in Milan, Italy. Atmos Environ 45:3522–3527. https://doi.org/10.1016/j.atmosenv.2011.04.008

Isley CF, Nelson PF, Taylor MP, Mani FS, Maata M, Atanacio A, Stelcer E, Cohen DD (2017) $PM_{2.5}$ and aerosol black carbon in Suva, Fiji. Atmos Environ 150:55–66. https://doi.org/10.1016/j.atmosenv.2016.11.041

Jaffe D, Putz J, Hof G, Hof G, Hee J, Lommers-Johnson DA, Gabela F, Fry JL, Ayres B, Kelp M, Minsk M (2015) Diesel particulate matter and coal dust from trains in the Columbia River Gorge, Washington State, USA. Atmos Pollut Res 6:946–952. https://doi.org/10.1016/j.apr.2015.04.004

Ji D, Li L, Pang B, Xue P, Wang L, Wu Y, Zhang H, Wang Y (2017) Characterization of black carbon in an urban-rural fringe area of Beijing. Environ Pollut 223:524–534. https://doi.org/10.1016/j.envpol.2017.01.055

Koelmans AA, Jonker MTO, Cornelissen G, Bucheli TD, Van Noort PCM, Gustafsson Ö (2006) Black carbon: the reverse of its dark side. Chemosphere 63:365–377. https://doi.org/10.1016/j.chemosphere.2005.08.034

Krasowsky TS, McMeeking GR, Wang D, Sioutas C, Ban-Weiss GA (2016) Measurements of the impact of atmospheric aging on physical and optical properties of ambient black carbon particles in Los Angeles. Atmos Environ 142:496–504. https://doi.org/10.1016/j.atmosenv.2016.08.010

Krecl P, Johansson C, Targino AC, Ström J, Burman L (2017) Trends in black carbon and size-resolved particle number concentrations and vehicle emission factors under real-world conditions. Atmos Environ 165:155–168. https://doi.org/10.1016/j.atmosenv.2017.06.036

Lara LL, Artaxo P, Martinelli LA, Camargo PB, Victoria RL, Ferraz ESB (2005) Properties of aerosols from sugar-cane burning emissions in Southeastern Brazil. Atmos Environ 39:4627–4637. https://doi.org/10.1016/j.atmosenv.2005.04.026

Louwies T, Nawrot T, Cox B, Dons E, Penders J, Provost E, Panis LI, De Boever P (2015) Blood pressure changes in association with black carbon exposure in a panel of healthy adults are independent of retinal microcirculation. Environ Int 75:81–86. https://doi.org/10.1016/j.envint.2014.11.006

Lyamani H, Olmo FJ, Foyo I, Alados-Arboledas L (2011) Black carbon aerosols over an urban area in South-Eastern Spain: changes detected after the 2008 economic crisis. Atmos Environ 45:6423–6432. https://doi.org/10.1016/j.atmosenv.2011.07.063

Ma J, Tang J, Li S-M, Jacobson MZ (2003) Size distributions of ionic aerosols measured at Waliguan observatory: implication for nitrate gas-to-particle transfer processes in the free troposphere. J Geophys Res 108:4541. https://doi.org/10.1029/2002JD003356

Mao Y-H, Liao H (2016) Impacts of meteorological parameters and emissions on decadal, interannual, and seasonal variations of atmospheric black carbon in the Tibetan Plateau. Adv Clim Chang Res 7:123–131. https://doi.org/10.1016/j.accre.2016.09.006

Marinoni A, Cristofanelli P, Laj P, Duchi R, Calzolari F, Decesari S, Sellegri K, Vuillermoz E, Verza GP, Villani P, Bonasoni P (2010) Aerosol mass and black carbon concentrations, a two year record at NCO-P (5079 m, Southern Himalayas). Atmos Chem Phys 10:8551–8562. https://doi.org/10.5194/acp-10-8551-2010

Markowicz KM, Ritter C, Lisok J, Makuch P, Stachlewsk IS, Cappelletti D, Mazzola M, Chilinski MT (2017) Vertical variability of aerosol single-scattering albedo and equivalent black carbon concentration based on in-situ and remote sensing techniques during the iAREA campaigns in Ny-Ålesund. Atmos Environ 164:431–447. https://doi.org/10.1016/j.atmosenv.2017.06.014

Ming J, Xiao C, Sun J, Kang S, Bonasoni P (2010) Carbonaceous particles in the atmosphere and precipitation of the Nam Co region, Central Tibet. J Environ Sci 22:1748–1756. https://doi.org/10.1016/S1001-0742(09)60315-6

Naoe H, Hasegawa S, Heintzenberg J, Okada K, Uchiyama A, Zaizen Y, Kobayashi E, Yamazaki A (2009) State of mixture of atmospheric submicrometer black carbon particles and its effect on particulate light absorption. Atmos Environ 43:1296–1301. https://doi.org/10.1016/j.atmosenv.2008.11.031

Ni M, Huang J, Lu S, Li X, Yan J, Cen K (2014) A review on black carbon emissions, worldwide and in China. Chemosphere 107:83–93. https://doi.org/10.1016/j.chemosphere.2014.02.052

Pani SK, Verma S (2014) Variability of winter and summertime aerosols over eastern India urban environment. Atmos Res 137:112–124. https://doi.org/10.1016/j.atmosres.2013.09.014

Patel MM, Chillrud SN, Correa JC, Feinberg M, Hazi Y, Deepti KC, Prakash S, Ross JM, Levy D, Kinney PL (2009) Spatial and temporal variations in traffic-related particulate matter at New York City high schools. Atmos Environ 43:4975–4981. https://doi.org/10.1016/j.atmosenv.2009.07.004

Quintana PJE, Dumbauld JJ, Garnica L, Chowdhury MZ, Velascosoltero J, Mota-Raigoza A, Flores D, Rodríguez E, Panagon N, Gamble J, Irby T, Tran C, Elder J, Galaviz VE, Hoffman L, Zavala M, Molina LT (2014) Traffic-related air pollution in the community of San Ysidro, CA, in relation to northbound vehicle wait times at the US-Mexico border port of entry. Atmos Environ 88:353–361. https://doi.org/10.1016/j.atmosenv.2014.01.009

Rakowska A, Wong KC, Townsend T, Chan KL, Westerdahl D, Ng S, Močnik G, Drinovec L, Ning Z (2014) Impact of traffic volume and composition on the air quality and pedestrian exposure in urban street canyon. Atmos Environ 98:260–270. https://doi.org/10.1016/j.atmosenv.2014.08.073

Ramanathan V, Carmichael G (2008) Global and regional climate changes due to black carbon. Nat Geosci 1(4):221–227. https://doi.org/10.1038/ngeo156

Raysoni AU, Sarnat JA, Sarnat SE, Garcia JH, Holguin F, Luèvano SF, Li W-W (2011) Binational school-based monitoring of traffic-related air pollutants in El Paso, Texas (USA) and ciudad Juárez, Chihuahua (México). Environ Pollut 159:2476–2486. https://doi.org/10.1016/j.envpol.2011.06.024

Ruellan S, Cachier H (2001) Characterisation of fresh particulate vehicular exhausts near a Paris high flow road. Atmos Environ 35:453–468. https://doi.org/10.1016/S1352-2310(00)00110-2

Shrestha G, Traina JS, Swanston WC (2010) Black carbon's properties and role in the environment: a comprehensive review. Sustainability 2:294–320. https://doi.org/10.3390/su2010294

Srivastava AK, Bisht DS, Ram K, Tiwari S, Srivastava MK (2014) Characterization of carbonaceous aerosols over Delhi in Ganga basin: seasonal variability and possible sources. Environ Sci Pollut Res 21:8610–8619. https://doi.org/10.1007/s11356-014-2660-y

Takahama S, Russell LM, Shores CA, Marr LC, Zheng J, Levy M, Zhang R, Castillo E, Rodriguez-Ventura JG, Quintana PJE, Subramanian R, Zavala M, Molina LT (2014) Diesel vehicle and urban burning contributions to black carbon concentrations and size distributions in Tijuana, Mexico, during the Cal-Mex 2010 campaign. Atmos Environ 88:341–352. https://doi.org/10.1016/j.atmosenv.2013.09.057

Tan Y, Kwan M-P, Chai Y (2017) Examining the impacts of ethnicity on space-time behavior: evidence from the City of Xining, China. Cities 64:26–36. https://doi.org/10.1016/j.cities.2017.02.003

van der Zee SC, Fischer PH, Hoek G (2016) Air pollution in perspective: health risks of air pollution expressed in equivalent numbers of passively smoked cigarettes. Environ Res 148:475–483. https://doi.org/10.1016/j.envres.2016.04.001

Vedantham R, Norris G, Brown SG, Roberts P (2012) Combining continuous near–road monitoring and inverse modeling to isolate the effect of highway expansion on a school in Las Vegas. Atmos Pollut Res 3:105–111. https://doi.org/10.5094/APR.2012.010

Viidanoja J, Sillanpää M, Laakia J, Kerminen V-M, Hillamo R, Aarnio P, Koskentalo T (2002) Organic and black carbon in $PM_{2.5}$ and PM_{10}: 1 year of data from an urban site in Helsinki, Finland. Atmos Environ 36:3183–3193. https://doi.org/10.1016/S1352-2310(02)00205-4

Wang H, Shooter D (2005) Source apportionment of fine and coarse atmospheric particles in Auckland, New Zealand. Sci Total Environ 340:189–198. https://doi.org/10.1016/j.scitotenv.2004.08.017

Wang H, He Q, Chen Y, Kang Y (2014) Characterization of black carbon concentrations of haze with different intensities in Shanghai by a three-year field measurement. Atmos Environ 99:536–545. https://doi.org/10.1016/j.atmosenv.2014.10.025

Wang M, Xu B, Wang N, Cao J, Tie X, Wang H, Zhu C, Yang W (2016) Two distinct patterns of seasonal variation of airborne black carbon over Tibetan Plateau. Sci Total Environ 573:1041–1052. https://doi.org/10.1016/j.scitotenv.2016.08.184

Weichenthal S, Farrell W, Goldberg M, Joseph L, Hatzopoulou M (2014) Characterizing the impact of traffic and the built environment on near-road ultrafine particle and black carbon concentrations. Environ Res 132:305–310. https://doi.org/10.1016/j.envres.2014.04.007

Wu J, Duan D, Lu J, Luo Y, Wen X, Guo X, Boman BJ (2016a) Inorganic pollution around the Qinghai-Tibet Plateau: an overview of the current observations. Sci Total Environ 550:628–636. https://doi.org/10.1016/j.scitotenv.2016.01.136

Wu J, Lu J, Luo Y, Duan D, Zhang Z, Wen X, Min X, Guo X, Boman BJ (2016b) An overview on the organic pollution around the Qinghai-

Tibet plateau: the thought-provoking situation. Environ Int 97:264–272. https://doi.org/10.1016/j.envint.2016.09.019

Yoo H-J, Kim J, Yi S-M, Zoh K-D (2011) Analysis of black carbon, particulate matter, and gaseous pollutants in an industrial area in Korea. Atmos Environ 45:7698–7704. https://doi.org/10.1016/j.atmosenv.2011.02.049

Zhang H, Wang Z (2011) Advances in the study of black carbon effects on climate. Adv Clim Chang Res 2(1):23–30. https://doi.org/10.3724/SP.J.1248.2011.00023

Zhao S, Ming J, Xiao C, Sun W, Qin X (2012) A preliminary study on measurements of black carbon in the atmosphere of northwest Qilian Shan. J Environ Sci 24:152–159. https://doi.org/10.1016/S1001-0742(11)60739-0

Zhao S, Tie X, Long X, Cao J (2017) Impacts of Himalayas on black carbon over the Tibetan plateau during summer monsoon. Sci Total Environ 598:307–318. https://doi.org/10.1016/j.scitotenv.2017.04.101

Zhu C-S, Cao J-J, Hu T-F, Shen Z-X, Tie X-X, Huang H, Wang Q-Y, Huang R-J, Zhao Z-Z, Močnik G, Hansen ADA (2017) Spectral dependence of aerosol light absorption at an urban and a remote site over the Tibetan Plateau. Sci Total Environ 590–591:14–21. https://doi.org/10.1016/j.scitotenv.2017.03.057